

Water-Dependent Micromechanical and Rheological Properties of Silica Colloidal Crystals Studied by Nanoindentation

Francisco Gallego-Gómez,^{*,†} Víctor Morales-Flórez,[‡] Álvaro Blanco,[†] Nicolás de la Rosa-Fox,[§] and Cefe López[†]

[†]Instituto de Ciencia de Materiales de Madrid, ICMM (CSIC), C/Sor Juana Inés de la Cruz 3, 28049 Madrid, Spain

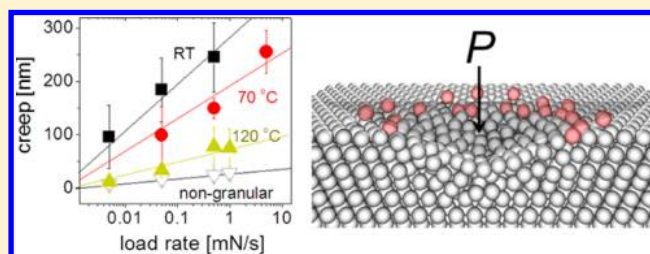
[‡]Instituto de Ciencia de Materiales de Sevilla, ICMS (CSIC-Universidad de Sevilla), Avenida Américo Vespucio, 49, 41092, Seville, Spain

[§]Departamento de Física de la Materia Condensada, Universidad de Cádiz, Avenida República Saharaui s/n, Puerto Real 11510, Cadiz, Spain

S Supporting Information

ABSTRACT: Here we show the suitability of nanoindentation to study in detail the micromechanical response of silica colloidal crystals (CCs). The sensitivity to displacements smaller than the submicrometer spheres size, even resolving discrete events and superficial features, revealed particulate features with analogies to atomic crystals. Significant robustness, long-range structural deformation, and large energy dissipation were found. Easily implemented temperature/rate-dependent nanoindentation quantified the paramount role of adsorbed water endowing silica CCs with properties of wet granular materials like viscoplasticity. A novel “nongranular” CC was fabricated by substituting capillary bridges with silica necks to directly test water-independent mechanical response. Silica CCs, as specific (nanometric, ordered) wet granular assemblies with well-defined configuration, may be useful model systems for granular science and capillary cohesion at the nanoscale.

KEYWORDS: Nanoindentation, colloidal crystals, capillary cohesion, energy dissipation, viscoplasticity, wet granular materials



Solid colloidal crystals (also referred to as artificial opals) have important applications in, for example, photonics, energy conversion, sensing, and as templates,^{1,2} for which diverse mechanical requirements are mandatory, so that the study of issues like the stability against deformation is essential. They are also used for modeling of atomic systems,^{3,4} where mechanical features may impart relevant information. However, mechanical testing of CCs is not well-established and very little is known about their mechanical properties and governing factors. CCs are ordered particulate materials formed by self-assembly of monodisperse spheres, whereby submicrometer silica spheres are particularly convenient to build inexpensive, high-quality face-centered-cubic (fcc) structures.⁵ In as-grown CCs, cohesion between colloidal spheres is just determined by short-range interparticle forces like van der Waals and electrostatic interactions.⁶ In the case of hydrophilic particles, capillarity becomes relevant as water uptaken from ambient moisture forms liquid bridges. In silica CCs, the presence of significant amount of physisorbed water (about 8 wt %⁷), leads to slightly nonclose packed fcc spheres arrangement, in which spheres are not in true contact but held together by water necks⁸ in a pendular state.⁹ The 335 nm spheres have an estimated separation of 12 nm.¹⁰ In granular materials, small amounts of liquid have a well-known effect on the mechanical properties via both capillary cohesion between grains and

increased interparticle friction.^{9,11} In these “wet” materials, grains arrangement (e.g., packing fraction, number of neighbors) and liquid distribution are decisive for the collective behavior^{11,12} but hard to identify. By contrast, silica CCs conforms a nearly ideal three-dimensional (3D) pseudogranular assembly with well-defined spheres and water configuration.⁸ Thus, understanding CCs mechanical properties is not only of obvious technological importance but it also can provide relevant insight into granular materials, which are ubiquitous in natural and industrial processes.

Macroscopic experimental techniques typically performed on granular matter are not suitable for the small colloidal samples. Conversely, nanoindentation allows the probing of a material by nano/micrometer displacements and it has been extensively used in continuous media,^{13–15} including nanoframes.^{16,17} However, its application to colloidal assemblies is restricted to a few studies on capped nanocrystals and supercrystals films^{18–20} and polymer-stabilized or sintered aggregates.^{21,22} Mechanics of bare colloidal crystals has been marginally researched, and nanoindentation has been just employed on them to assess strength increase upon pore filling^{23–25}

Received: July 6, 2012

Revised: August 7, 2012

Published: August 7, 2012

Here we used nanoindentation for reliable micromechanical characterization of CCs formed by bare silica spheres (without extrinsic ligands) (see Supporting Information text and Figure S1). Its slightly destructive character allowed good statistics in very small volumes whereas its sensitivity to deformations comparable to spheres size provided information about particulate features. Experiments on heated opals (up to 150 °C) in which water content was easily controlled elucidated the influence of capillary cohesion on the mechanical strength of the CC, measured by both indentation hardness (H) and modulus (E). Viscous behavior was revealed by the rheological properties investigated at varying loading rates (spanning 3 orders of magnitude) and different water contents. Finally, a novel type of CC whereby water did not contribute to cohesion was fabricated and characterized for direct comparison.

Nanoindentation at maximum penetration depths h_{\max} ranging from about $0.4 d_{111}$ to $18 d_{111}$ (d_{111} is the interplanar distance in the CC, 280 nm in our case), was performed to account for surface micromechanical features (involving only superficial spheres) as well as bulk ones (Supporting Information Figure S2). Scanning electron microscopy (SEM) images of the residual indents provided first insights into the opal response. Low-depth indents (Figure 1a) approached a

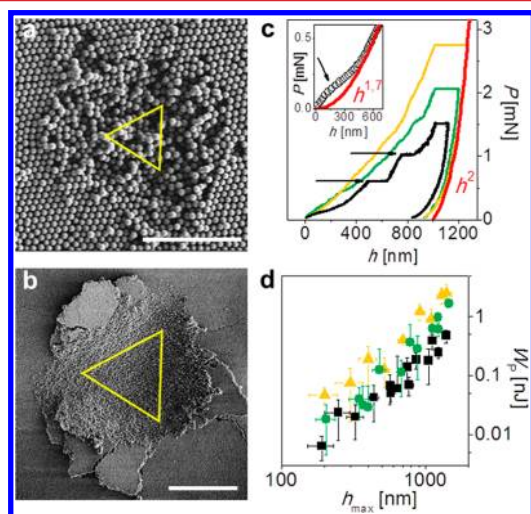


Figure 1. (a,b) SEM micrographs of residual indents at $h_{\max} = 500$ and 4600 nm (scale bars are 5 and $20 \mu\text{m}$), respectively. Yellow triangles delimit the intersection areas of the Berkovich indenter (at maximum penetration h_{\max}) with the surface plane. (c) Typical load-depth curves with $h_{\max} = 1000$ nm performed at different load rates (5 , 50 , and $500 \mu\text{N/s}$ – black, green, and orange lines, respectively). Two pop-in events, designated by arrows, are visible at the lowest rate. Inset: zoom-in of the loading curve at early penetration stage (rate of $50 \mu\text{N/s}$); the arrow indicates a characteristic initial displacement burst. Red curves are fitting power-law functions. (d) Plastic work (W_p) measured at load rates of 5 , 50 , and $500 \mu\text{N/s}$ (same colors as in panel c).

formless shape instead of the well-defined triaxial one typically let by Berkovich indenters in continuous materials^{13,15} and even in capped^{19–21} or sintered²² colloidal assemblies. This must be attributed to the highly incompressible CC structure (even nonclose-packed), which nearly isotropically accommodated the displaced volume over a region clearly exceeding the indented area and by uplifting individual spheres (pile-up). The dense crystalline arrangement of the CC probably has long force chains^{20,26} that may facilitate the transmission of deformation beyond the contact area through the structure.

These features were readily obtained with a simplified Monte Carlo simulation of loading (Supporting Information Figure S3). Deeper indents (above $h_{\max} \sim 3 \mu\text{m}$) exhibited recognizable triangular shape and pile-up of entire “chips” of assembled particles (Figure 1b).

Load (P)–depth (h) curves revealed that the deformation rate intrinsically affected the mechanical response (Figure 1c). Indeed, load curves became steeper at faster loading rates, denoting viscous behavior.^{14,19,27} The pronounced creep displacements during dwell time (over 100 nm) confirmed the occurrence of viscous flow under compression, which is characteristic of polymers²⁷ and also some polymer-bonded colloidal films,^{19,20} but was unexpected in our polymer-free system. Rather, this behavior recalls that of wet granular materials, which commonly exhibit increased time-dependence of the mechanical response due to the liquid between the grains.^{11,12} By analogy, the adsorbed water between the spheres may be responsible for the viscous behavior of the opal (see below). Interestingly, at the lowest loading rate abrupt displacements, even as large as 200 – 300 nm, were often observed at constant loads (pop-in events) denoting prompt sliding of planes in the crystalline structure.^{14,15} At higher rates, discontinuities became fewer or less pronounced.¹⁵ Upon unloading, as the pressure is released, some depth recovery demonstrated partial elastic recovery of the crystalline spheres assembly (Figure 1c). However, the plastic work (W_p) predominated over the elastic one (W_e), even at indentation depths as low as 100 nm, indicating that most of the structure deformation was irreversible. Unloading curves showed high reproducibility and well-defined h^2 -dependence (in accordance to the Oliver and Pharr model^{13,14}), allowing reliable quantification of both H and E to characterize the mechanical CC strength.

At early indentation stages (until ca. 500 nm) load curves demonstrated higher resistance of the CC to deformation (Figure 1c, inset). This suggests that inducing the initial dislocations in the ordered packing required more energy, whereas further penetration became easier in the progressively distorted structure. This transition sometimes appeared in the CC as a moderate displacement burst, typically within the first 300 nm (arrow in Figure 1c, inset), which agrees with the induction of dislocations in CCs by indenting a sharp needle about d_{111} .³ This behavior was consistent with the observed depth-dependence of H and E , which exhibited a pronounced drop within the initial 400 nm (Supporting Information Figure S4). These features bear similarity to the incipient plasticity observed in atomic crystals upon initiation of defect nucleation.¹⁵

CCs showed a remarkable ability to dissipate energy in form of plastic deformation. As shown in Figure 1d, W_p followed a power-law dependence with h_{\max} (with exponent of ~ 2.4). Moreover, the plastic work increased with the rate, indicating that energy was absorbed more efficiently during fast deformations. For sake of comparison, $W_p \sim 0.2$ nJ at $h_{\max} = 600$ nm (at maximum load of ~ 1 mN), which is comparable to the best absorbing polymer foams²⁸ and periodic epoxy nanoframes at similar strains.¹⁶ Energy dissipation in the CC may be enhanced by several factors such as the large number of bonds per sphere (12) to be broken, which is maximum in the fcc arrangement, and the long force chains in the dense crystalline structure, allowing the stress to span a large volume. Additional dissipation is likely induced by the viscosity of the thin interfacial water in the silica CC, which can be much

higher than that of bulk water.²⁹ The observed rate-dependence agrees with such viscous dissipative process.

At the lowest rate measured ($5 \mu\text{N/s}$), $H \sim 60 \text{ MPa}$ and $E \sim 2 \text{ GPa}$ in the bulk CC and increased at faster load/unload rates (Supporting Information Figure S4), confirming the time-dependence of the CC mechanical properties. These values, which are similar to hard polymers and capped colloidal films,^{18,20,21} are remarkably large given the lack of interparticle ligands. Apart from the positive effect of the structure crystallinity, which allows more homogeneous stress distribution,^{20,21} such robustness seems to be attributable to capillary cohesion between the hydrophilic silica spheres. This agrees with the reduced toughness measured in assemblies of hydrophobic spheres like polystyrene opals²⁴ ($H \sim 10 \text{ MPa}$ and $E \sim 0.5 \text{ GPa}$ at 10% of the sample thickness). To prove this issue, we implemented temperature-dependent nanoindentation on silica CCs, which led, within the data dispersion, to clear leveling of the loading curves (Supporting Information Figure S5), indicating that the structure became more compliant.

H and E exhibited an overall reduction with T , reaching a 2-fold drop above $100 \text{ }^\circ\text{C}$ (Figure 2a,b). This trend agreed with

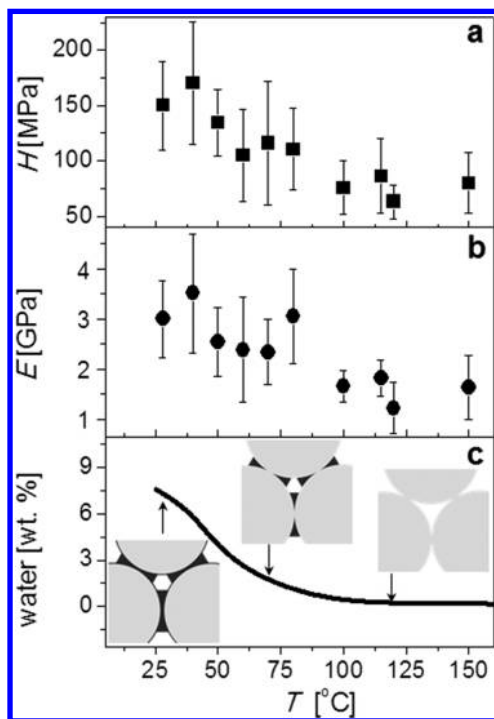


Figure 2. Temperature-dependence of H (a) and E (b), both measured at $h_{\text{max}} = 600 \text{ nm}$, and content of adsorbed water in the CC (c). Sketches in (c) depict the distribution of water (black) between the opal spheres (gray) at $T = 28, 70$, and $120 \text{ }^\circ\text{C}$ according to data of ref 8 (proportions are maintained).

the decrease of adsorbed water contained in the CC, as measured by thermogravimetry (Figure 2c), which leads to progressive shrinkage of the water necks between spheres⁸ until virtually complete removal at about $100 \text{ }^\circ\text{C}$. Such correlation is a quantitative proof that in this range the higher the water content, the higher the capillary cohesion in the CC, as it occurs in wet granular materials. Without adsorbed water ($T > 100 \text{ }^\circ\text{C}$), the “dry” CC still kept stable with nonvanishing H and E values attributable to van der Waals attraction between

spheres (which increased upon water desorption as spheres approached close contact⁸) and remaining interparticle friction. The stability of the dry CC is in accordance with the nonvanishing pull-off forces measured between silica surfaces at 0% humidity.³⁰ Between 100 and $150 \text{ }^\circ\text{C}$, interparticle forces were expected not to vary as physisorbed water has been already removed and spheres cannot further approach, which agreed with the constancy of H and E values in this range. Temperature-induced changes in the spheres toughness can be disregarded as silica properties barely changed with temperature.¹⁴

As mentioned above, the unexpected viscous response was conjectured to be caused by the adsorbed water between CC spheres. To demonstrate this point, we studied the rheological properties of heated samples, that is, at decreasing water contents. Creep experiments at varying indentation rate and temperature allowed evaluation of the viscoplasticity (rather than viscoelasticity, given the predominantly irreversible deformation). As a general rule, the larger the viscous response, the larger the creep displacement Δh and its rate-dependence.^{14,19,27} Regarding the latter aspect, as long as viscous response occurs simultaneously to loading, the creep depends on the degree of accommodation of the system to the imposed deformation when the dwell time begins. At low indentation rates, the viscous flow is mostly dissipated during the gentle loading, so that Δh is small and exhibits slow dynamics due to a long-term contribution associated to shear deformation. At high rates, most of the deformation cannot be accommodated during the rapid loading but during the dwell time, leading to large and fast creep.

Rate-dependent experiments confirmed the marked viscoplastic character of the silica CC at room temperature (RT), as Δh strongly increased with the loading rate (Figure 3a) and its dynamics progressively speeded up (normalized creeps in Figure 3b). Figure 3a also shows that, as water was removed from the CC by increasing T , the rate dependence obviously reduced, which evidence that the viscoplastic response tends to vanish in the dry CC, as hypothesized. The correlation between water and creep was further supported by the decrease of Δh , at constant rate, with T (Figure 3c) in close analogy to the water content (Figure 2c). Such drop with temperature drastically differed from the typically thermally activated creep observed in polymers and confirms the distinct nature of (at least most of) the viscous response in the CC. However, some remnant creep was measured in the dry CC (at $T > 100 \text{ }^\circ\text{C}$), which, by growing T , even exhibited a slight increase (Figure 3c) and somewhat faster dynamics (Figure 3d).

In wet granular materials, time-dependent mechanical behavior has been assigned to slow flow of the liquid over the grains surface allowed by enough connectivity of the capillary network.^{11,12} Characteristic times of tens of seconds have been estimated for water,¹² which roughly agree with our creep measurements. Evidence in silica CCs of both interconnected water distribution and water transport has recently been reported,^{8,10} so the latter could indeed significantly affect the rheological properties similarly to wet granular matter. On the other hand, the residual viscous response in the dry CC rather resembles that observed in dry granular materials, in which, although less pronouncedly than in wet conditions, dense granular flows can behave like viscous liquids.³¹

For purposes of direct comparison, we aimed to fabricate a CC in which the interparticle cohesion does not depend on

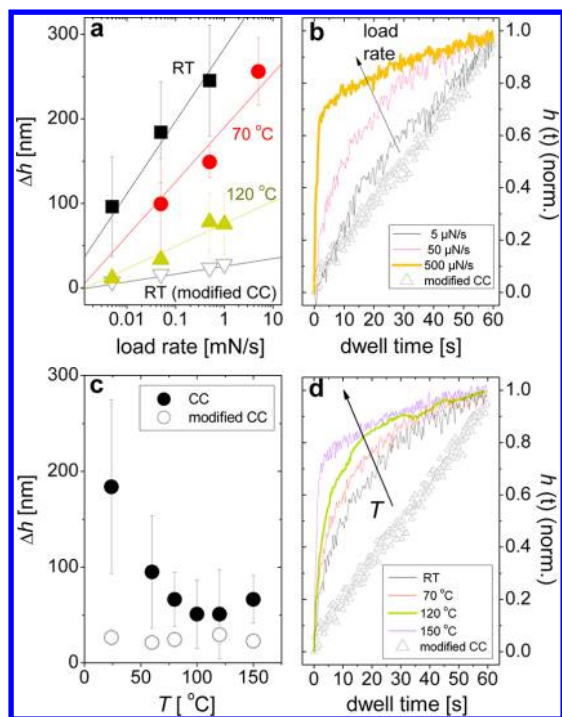


Figure 3. (a) Creep displacement Δh after dwell time of 60 s as function of the load rate (symbols) and linear fits (lines), measured in CCs at RT, 70 and 120 °C, and in the CVD-modified CC (at RT). (b) Normalized transient creep $h(t)$ measured at RT in CCs at 5, 50, and 500 $\mu\text{N/s}$ and in the CVD-modified CC (at 50 $\mu\text{N/s}$). (c) Δh as a function of the sample temperature (rate of 50 $\mu\text{N/s}$). (d) Normalized $h(t)$ measured at 50 $\mu\text{N/s}$ in CCs at RT, 50, 120, and 150 °C and in the CVD-modified CC (at RT). All experiments were performed at constant load $P = 1.5$ mN.

adsorbed water. Therefore, the silica CC was modified with customized chemical vapor deposition (CVD) to transform the capillary bridges between spheres into silica necks without additional silica infiltration. As a result, we obtained a monolithic nanoframe with rigid interparticle bonds whereby the presence (and flow) of adsorbed water is not avoided but its influence on the mechanical cohesion. Thus, this “nongranular” replica represents a useful limit of water-independent mechanical response in the CC. Nanoindentation experiments performed on it showed insignificant thermal dependence in H and E (not shown) and nearly negligible creep displacement with poor dependence on both rate (Figure 3a) and T (Figure 3c). The creep dynamics, which virtually remained unchanged in all cases, was much slower than that in unmodified CCs (Figure 3b,d). These features drastically contrast with those obtained in the bare silica CC and verify the large influence on the CC mechanics assigned to water. In particular, the distinct creep behaviors revealed the intrinsically different response of a nongranular CC (rigid interparticle bonds) versus a bare CC (with loosely bonded particles) and, in the latter case, of a wet vs a dry CC. This provides a simple way to characterize a colloidal assembly and distinguish the nature of the interparticle bonds by a few creep experiments.

In conclusion, an unprecedented analysis of the micro-mechanical response of bare silica colloidal crystals has been performed by depth-, rate-, and temperature-dependent nanoindentation. The specific characteristics of silica CCs, including crystallinity, submicrometer-sized particles, and particulate character, provided interesting links to features of

both atomic crystals and granular materials. In particular, the presence of adsorbed water between the constitutive spheres bestowed remarkable properties of wet granular media, as easily probed by nanoindentation during heat-controlled desorption. Unexpectedly, wet CCs showed pronounced viscous behavior, which was mainly attributed to flow of adsorbed water between spheres. Different aspects remain open, such as the influence of the assumed nonclose spheres packing in the CC, which should consider local deviations, spheres surface roughness and the arrangement evolution upon compression and water desorption. Some creep features are not fully understood like the dry CC behavior, which appears to depend on temperature. An efficient distinction between water- and temperature-dependent contributions to mechanics will give deeper insight. Direct comparison with a nongranular replica already provided straightforward verification of the prominent role of water in the bare CC mechanics. Nanoindentation on hydrophobic (polymer) CC or under vacuum will further help isolate the water-related issues. In summary, this work proves the suitability of nanoindentation to explore mechanical features of CCs, which offer a versatile 3D model system with well-defined water/particles morphology and wide choice of size, material and postproduction techniques like annealing or infiltration.

■ ASSOCIATED CONTENT

📄 Supporting Information

Experimental methods (colloidal crystals fabrication and nanoindentation procedure), Monte Carlo simulation, depth-dependent hardness and Young modulus, and temperature-dependent load-depth measurements. This material is available free of charge via the Internet at <http://pubs.acs.org>.

■ AUTHOR INFORMATION

Corresponding Author

*E-mail: francisco.gallego@icmm.csic.es.

Notes

The authors declare no competing financial interest.

■ ACKNOWLEDGMENTS

F.G.-G. and V.M.-F. were supported by the JAE Postdoctoral Program from the CSIC. This work was supported by EU FP7 NoE Nanophotonics4-Energy (Grant 248855), the Spanish MICINN (CSD2007-0046, Nanolight.es), MAT2009-07841 (GLUSFA), Comunidad de Madrid S2009/MAT-1756 (PHAMA) and Junta de Andalucía (TEP-0115) projects. The authors thank M. C. Jiménez de Haro for SEM characterization at the ICMS.

■ REFERENCES

- (1) Galisteo-López, J. F.; Ibisate, M.; Sapienza, R.; Froufe-Perez, L. S.; Blanco, A.; Lopez, C. *Adv. Mater.* **2011**, *23*, 30–69.
- (2) Zhao, Y.; Xie, Z.; Gu, H.; Zhu, C.; Gu, Z. *Chem. Soc. Rev.* **2012**, *41*, 3297–3317.
- (3) Schall, P.; Cohen, I.; Weitz, D. A.; Spaepen, F. *Nature* **2006**, *440*, 319–323.
- (4) Ganapathy, R.; Buckley, M. R.; Gerbode, S. J.; Cohen, I. *Science* **2010**, *327*, 445–448.
- (5) Miguez, H.; Meseguer, F.; López, C.; Mifsud; Moya, J. S.; Vazquez, L. *Langmuir* **1997**, *13*, 6009.
- (6) Butt, H. J.; Kappl, M. *Surface and Interfacial Forces*; Wiley-Vch Verlag: Weinheim, 2010.

- (7) Gallego-Gómez, F.; Blanco, A.; Golmayo, D.; López, C. *Langmuir* **2011**, *27*, 13992–13995.
- (8) Gallego-Gómez, F.; Blanco, A.; Canalejas-Tejero, V.; López, C. *Small* **2011**, *7*, 1838–1845.
- (9) Mitarai, N.; Nori, F. *Adv. Phys.* **2006**, *55*, 1–45.
- (10) Gallego-Gómez, F.; Blanco, A.; D.; López, C. *J. Phys. Chem. C* **2012**, DOI: 10.1021/jp303821u.
- (11) Herminghaus, S. *Adv. Phys.* **2005**, *54*, 221–261.
- (12) Kohonen, M. M.; Geromichalos, D.; Scheel, M.; Schier, C.; Herminghaus, S. *Physica A* **2004**, *339*, 7–15.
- (13) Oliver, W. C.; Pharr, G. M. *J. Mater. Res.* **1992**, *7*, 1564–1583.
- (14) Fischer-Cripps, A. C. *Nanoindentation*; Springer: New York, 2002.
- (15) Schuh, C. A. *Mater. Today* **2006**, *9*, 32–40.
- (16) Lee, J. H.; Wang, L.; Kooi, S.; Boyce, M. C.; Thomas, E. L. *Nano Lett.* **2010**, *10*, 2592–2597.
- (17) Tan, J. C.; Cheetham, A. K. *Chem. Soc. Rev.* **2011**, *40*, 1059–1080.
- (18) Klajn, R.; Bishop, J. M. B.; Fialkowski, M.; Paszewski, M.; Campbell, C. J.; Gray, T. P.; Grzybowski, B. A. *Science* **2007**, *316*, 261–264.
- (19) Lee, D.; Jia, S.; Banerjee, S.; Bevk, J.; Herman, I. P.; Kysar, J. W. *Phys. Rev. Lett.* **2007**, *98*, 026103.
- (20) Tam, E.; Podsiadlo, P.; Shevchenko, E.; Ogletree, D. F.; Delplancke-Ogletree, M. P.; Ashby, P. D. *Nano Lett.* **2010**, *10*, 2363–2367.
- (21) Roth, M.; Schilde, C.; Lellig, P.; Kwade, A.; Auernhammer, G. K. arXiv:1102.4233v2 (accessed May 12, 2012).
- (22) Yaghoubi, H.; Taghavinia, N.; Alamdari, E. K.; Volinsky, A. A. *ACS Appl. Mater. Interfaces* **2010**, *2*, 2629–2636.
- (23) Miguez, H.; Tetreault, N.; Hatton, B.; Yang, S. M.; Perovic, D.; Ozin, G. A. *Chem. Commun.* **2002**, *22*, 2736–2737.
- (24) Wang, J.; Wen, Y.; Ge, H.; Sun, Z.; Zheng, Y.; Song, Y.; Jiang, L. *Macromol. Chem. Phys.* **2006**, *207*, 596–604.
- (25) Dafinone, M. I.; Feng, G.; Brugarolas, T.; Tettey, K. E.; Lee, D. *ACS Nano* **2011**, *5*, 5078–5087.
- (26) Geng, J.; Howell, D.; Longhi, E.; Behringer, R. P.; Reydellet, G.; Vanel, L.; Clément, E.; Luding, S. *Phys. Rev. Lett.* **2001**, *87*, 035506.
- (27) Tweedie, A.; Van Vliet, K. J. *J. Mater. Res.* **2006**, *21*, 1576–1589.
- (28) Gibson, L. J.; Ashby, M. F. *Cellular solids*; Cambridge University Press: Cambridge, 1997.
- (29) Goertz, M. P.; Houston, J. E.; Zhu, X. Y. *Langmuir* **2007**, *23*, 5491–5497.
- (30) Xiao, X.; Qian, L. *Langmuir* **2000**, *16*, 8153–8158.
- (31) Forterre, Y.; Pouliquen, O. *Annu. Rev. Fluid Mech.* **2008**, *40*, 1–24.